This article is a *Plant Cell* Advance Online Publication. The date of its first appearance online is the official date of publication. The article has been edited and the authors have corrected proofs, but minor changes could be made before the final version is published. Posting this version online reduces the time to publication by several weeks.

EARLY FLOWERING4 Recruitment of EARLY FLOWERING3 in the Nucleus Sustains the *Arabidopsis* Circadian Clock [W][OA]

Eva Herrero,[a,1,2] Elsebeth Kolmos,[a,1,3] Nora Bujdoso,[a] Ye Yuan,[b] Mengmeng Wang,[b] Markus C. Berns,[a] Heike Uhlworm, [a] George Coupland,[a] Reena Saini,[c] Mariusz Jaskolski,[c] Alex Webb,[d] Jorge Gonçalves,[b] and Seth J. Davis[a,4]

[a] Max Planck Institute for Plant Breeding Research, D-50829 Cologne, Germany
[b] Department of Engineering, University of Cambridge, Cambridge CB2 1PZ, United Kingdom
[c] Department of Crystallography, Faculty of Chemistry, Adam Mickiewicz University, 60-780 Poznan, Poland
[d] Department of Plant Sciences, University of Cambridge, Cambridge CB2 3EA, United Kingdom

The plant circadian clock is proposed to be a network of several interconnected feedback loops, and loss of any component leads to changes in oscillator speed. We previously reported that *Arabidopsis thaliana EARLY FLOWERING4* (*ELF4*) is required to sustain this oscillator and that the *elf4* mutant is arrhythmic. This phenotype is shared with both *elf3* and *lux*. Here, we show that overexpression of either *ELF3* or *LUX ARRHYTHMO* (*LUX*) complements the *elf4* mutant phenotype. Furthermore, ELF4 causes ELF3 to form foci in the nucleus. We used expression data to direct a mathematical position of *ELF3* in the clock network. This revealed direct effects on the morning clock gene *PRR9*, and we determined association of ELF3 to a conserved region of the *PRR9* promoter. A *cis*-element in this region was suggestive of ELF3 recruitment by the transcription factor LUX, consistent with both *ELF3* and *LUX* acting genetically downstream of *ELF4*. Taken together, using integrated approaches, we identified ELF4/ELF3 together with LUX to be pivotal for sustenance of plant circadian rhythms.

INTRODUCTION

Adaptation of physiological and metabolic processes to daily changes in the environment is advantageous for sessile organisms, such as plants, because it enhances fitness and growth (Dodd et al., 2005). An internal circadian clock conveys this adaptation by providing timing information to synchronize to the diurnal cycle. This clock thus creates a mechanism to anticipate changes in light and temperature (Harmer, 2009). These external signals are termed "zeitgebers" and reset the clock at dawn (McWatters et al., 2000; Hicks et al., 2001). As a consequence, numerous processes are diurnally regulated, and these include global transcript accumulation, hormone signaling, photosynthesis, hypocotyl elongation, and plant–pathogen interactions (Davis and Millar, 2001; Hanano et al., 2006; Covington et al., 2008; Michael et al., 2008; Roden and Ingle, 2009; Graf et al., 2010; Li et al., 2011).

In *Arabidopsis thaliana*, extensive research on the molecular genetics of the circadian components, together with mathematical approaches, defined models of the circadian clock network (Zeilinger et al., 2006; Pokhilko et al., 2010). In the three-loop model, several transcription-translation feedback loops cause daily oscillations of transcript and protein accumulation of interlocked components. The core loop consists of the two partially redundant Myb-like transcription factors, *CIRCADIAN CLOCK ASSOCIATED1* (*CCA1*) and *LATE ELONGATED HYPOCOTYL* (*LHY*), whose expression peaks in the morning. The daytime accumulation of these factors leads to direct transcriptional suppression of the pseudo response regulator (PRR) *TIMING OF CAB EXPRESSION1* (*TOC1*). As *CCA1*/*LHY* expression declines over the day, this repression is released, which allows for highest *TOC1* transcript accumulation at night (Alabadí et al., 2001; Locke et al., 2006; Zeilinger et al., 2006; Ding et al., 2007). Coupled to this core oscillator is the expression of the *TOC1*-related *PRR9* and *PRR7*, repressor proteins that are in a positive-negative feedback with CCA1 and LHY (Locke et al., 2006; Zeilinger et al., 2006; Nakamichi et al., 2010). Similarly, the evening-expressed *GIGANTEA* (*GI*) positively regulates *TOC1* expression and contributes at least partially to the function of the mathematically defined clock component *Y* (Alabadí et al., 2001; Locke et al., 2006; Zeilinger et al., 2006; Ding et al., 2007). Taken together, much of the interconnected feedback loop appears to have been described at a molecular-genetic level of understanding.

One interesting mathematical feature derived from the three-loop mathematical models is the prediction that mutations in any of the above genes will cause a change in circadian periodicity, and this is indeed observed physiologically (Ding et al., 2007). As such, no single gene in the currently defined core oscillator is

[1] These authors contributed equally to this work.
[2] Current address: MRC National Institute for Medical Research, The Ridgeway, Mill Hill, London NW7 1AA, United Kingdom.
[3] Current address: Section of Cell and Developmental Biology, University of California San Diego, La Jolla, CA 92093.
[4] Address correspondence to davis@mpipz.mpg.de.
The author responsible for distribution of materials integral to the findings presented in this article in accordance with the policy described in the Instructions for Authors (www.plantcell.org) is: Seth J. Davis (davis@mpipz.mpg.de).
[W]Online version contains Web-only data.
[OA]Open Access articles can be viewed online without a subscription.
www.plantcell.org/cgi/doi/10.1105/tpc.111.093807

required for sustaining circadian rhythms. In stark contrast, there is a small group of clock loci in which mutations lead to inability to sustain circadian oscillations: *EARLY FLOWERING4* (*ELF4*) and *ELF3*, which code for sequence-unrelated proteins with no known functional domains, and the GARP transcription factor *LUX ARRHYTHMO* (*LUX*)/*PHYTOCLOCK1* (Hazen et al., 2005; Onai and Ishiura, 2005; McWatters et al., 2007; Thines and Harmon, 2010). These three genes are coexpressed, with peak transcript levels around dusk (Liu et al., 2001; Doyle et al., 2002; Onai and Ishiura, 2005).

Mutations at the *ELF4*, *ELF3*, and *LUX* loci lead to many similar phenotypic and molecular defects. Importantly, any respective single loss-of-function mutation leads to oscillator arrest at subjective dusk, both under constant light (LL) and in darkness (DD) (Hicks et al., 1996; Doyle et al., 2002; Hazen et al., 2005; Onai and Ishiura, 2005; McWatters et al., 2007; Thines and Harmon, 2010). A mechanism for this has started to be elucidated. Specifically, LUX has been recently proposed as a repressor targeting *PRR9* (Helfer et al., 2011). Similarly, it has been shown that the evening-expressed *ELF4* is a genetic repressor of *PRR9* (as well as *PRR7* and *GI*; Kolmos and Davis, 2007; Kolmos et al., 2009). ELF3 has also now been proposed to repress *PRR9* transcript accumulation (Dixon et al., 2011; Kolmos et al., 2011). A further common phenotype of the *elf3*, *elf4*, and *lux* mutants includes reduced levels of morning genes *CCA1* and *LHY* and elevated levels of *TOC1*, as well as defective photoperiodism with relation to flowering time (Schaffer et al., 1998; Fowler et al., 1999; Davis, 2002; Onai and Ishiura, 2005; McWatters et al., 2007; Thines and Harmon, 2010). Taken together, evening-expressed *ELF4*, *ELF3*, and *LUX* appear to act on the morning loop.

We previously reported structural modeling that predicts ELF4 as a ligand that activates a transcriptional repressor (Kolmos et al., 2009). ELF3 protein was reported to be nuclear localized, but it possesses no structural similarity to known functional domains (Hicks et al., 2001; Liu et al., 2001). The biochemical activity of ELF3 is therefore unclear. Finally, LUX has bona fide DNA binding activity and can directly bind to a *cis*-element in the *PRR9* promoter (Helfer et al., 2011). Collective considerations of the above data led us to hypothesize that *ELF4*, *ELF3*, and *LUX* are components of the same node within the clock network. In this study, we took a multidisciplinary approach to identify and characterize these clock factors as members of a dusk complex that works as a repressor to sustain rhythms of the circadian oscillator.

RESULTS

ELF3 and ELF4 Genetically and Physically Interact

Our previous findings that ELF4 resembles a ligand molecule (Kolmos et al., 2009) and that *ELF3* is genetically a repressor that must be activated (Kolmos et al., 2011) led us to hypothesize that *ELF3* and *ELF4* act in the same pathway. To test this, we generated the double loss-of-function mutant, *elf3-4 elf4-1*, and analyzed the rhythmic activity of the *CCA1* promoter using the luciferase (*LUC*) reporter *CCA1:LUC*. Under diurnal light-dark (LD) conditions, we found that *CCA1:LUC* expression in *elf3-4 elf4-1* was strongly reduced compared with the wild type (Figure 1A). Furthermore, in the *elf3-4* single and in the *elf3-4 elf4-1* double mutant, *CCA1:LUC* expression was similar and reduced compared with *elf4-1* (Figure 1B), which is consistent with *ELF3* being downstream of *ELF4* in the same genetic pathway.

To analyze further the epistatic relationship between these two *ELF* genes, and bypass their arrhythmic mutant phenotypes, we generated double mutants combining the loss of function of one and the overexpression of the other and analyzed circadian rhythms of *LHY:LUC* under LL. In the wild type, *LHY:LUC* expression displayed a circadian rhythm peaking in the early morning. Consistent with previous studies (Kikis et al., 2005; McWatters et al., 2007), both the *elf3-4* and *elf4-1* single mutants displayed marginal *LHY:LUC* activity and were arrhythmic (Figures 1C and 1D). Both the overexpression of *ELF3* (*ELF3-OX*) and *ELF4* (*ELF4-OX*) produced a long circadian period (Figures 1C and 1D), as previously described (Covington et al., 2001; McWatters et al., 2007). Similar to *elf3-4*, the *elf3-4 ELF4-OX* double mutant displayed dramatically attenuated *LHY:LUC* expression and no circadian rhythms, as seen in the *elf3-4* single mutant (Figure 1C). Thus, *ELF4* overexpression has no effect on the *elf3-4* phenotype. In stark contrast, *elf4-1 ELF3-OX* regained overt *LHY:LUC* bioluminescence and rhythmic activity, relative to the single *elf4-1* phenotype (Figure 1D; see Supplemental Figure 1A online). We then confirmed the rescue of the *elf4-1* phenotype by *ELF3* overexpression and tested the circadian rhythms for the *COLD, CIRCADIAN RHYTHM, AND RNA BINDING2* (*CCR2*) reporter in *elf4-1 ELF3-OX*. We found that *elf4-1 ELF3-OX* had rhythmic expression of *CCR2:LUC* both under LL and in DD (Figures 1E and 1F; see Supplemental Figures 1B and 1C online). Thus, we concluded that *ELF3* is genetically downstream of *ELF4*.

We then tested if ELF3 and ELF4 physically interact by the yeast two-hybrid assay (Y2H) and found that full-length ELF4 interacts with full-length ELF3 (Figure 2A). This was in accordance with a recent report on ELF4 and ELF3 interaction by Nusinow et al. (2011). Subsequently, we confirmed this interaction in planta by fluorescence resonance energy transfer (FRET) by coexpression of ELF3-CYAN FLUORESCENT PROTEIN (ELF3-CFP) and YELLOW FLUORESCENT PROTEIN-ELF4 (YFP-ELF4). Efficiency of FRET from the CFP to the YFP fluorophores was assayed by YFP photobleaching. As a negative control, we used RED FLUORESCENT PROTEIN-CFP (RFP-CFP) and YFP-RFP fusions. When YFP-ELF4 and ELF3-CFP were coexpressed, we found that the FRET efficiency was 52.4% $\pm$ 10.6%, while for the negative controls YFP-RFP with ELF3-CFP and YFP-ELF4 with RFP-CFP, the FRET efficiency was much lower (2.0% $\pm$ 2.3% and 3.5% $\pm$ 2.6%, respectively; Figure 2B). Thus, we demonstrated that ELF4 associates with ELF3 in planta.

Different domains of ELF3 are required for given protein interactions with other clock and light-signaling components (Liu et al., 2001; Yu et al., 2008). In the Y2H assay, we used a series of ELF3 deletion fragments and identified the ELF3 middle domain (ELF3M, residues 261 to 484) as the element required for interaction with ELF4 (Figure 2A). Note that only the constructs containing ELF3M (ELF3NM, ELF3M, and ELF3MC) led to viable yeast, whereas ELF3N and ELF3C did not. Subsequently, we confirmed the association between the middle region of ELF3

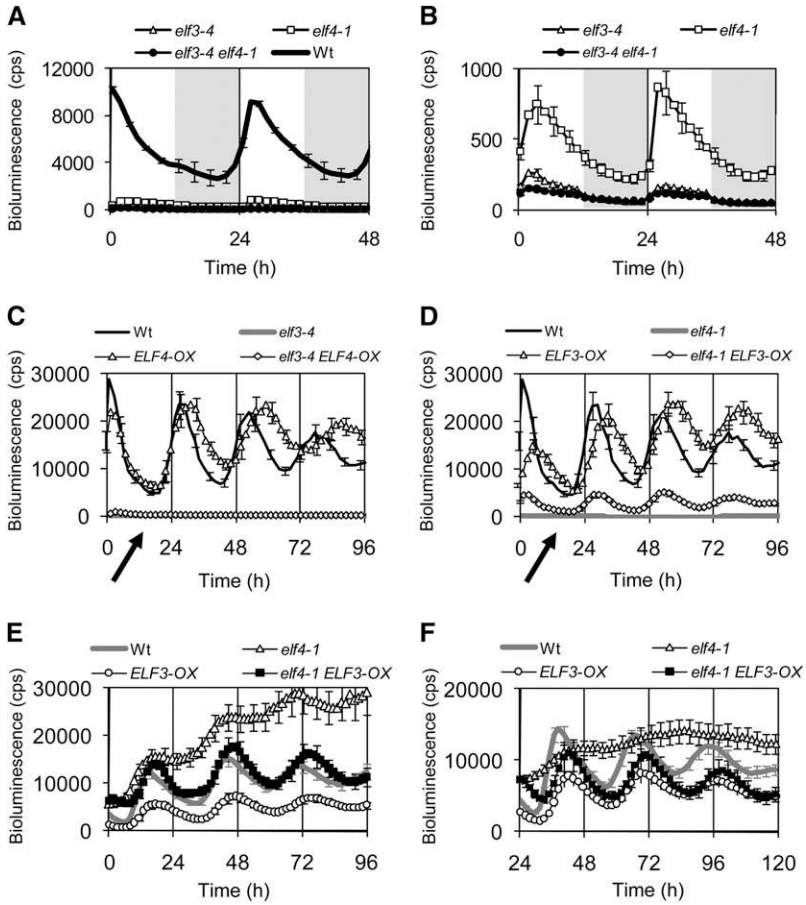

Figure 1. *ELF3* Is Downstream of *ELF4*.

(A) and **(B)** *CCA1*:*LUC* under LD (12 h light/12 h dark). *CCA1*:*LUC* expression was severely reduced in *elf3-4*, *elf4-1*, and *elf3-4 elf4-1* compared with the wild type (Wt). Note the different resolutions of the *y* axes and the lack of driven *CCA1*:*LUC* oscillations in *elf3-4* and *elf3-4 elf4-1*.

(C) and **(D)** Bioluminescence of *LHY*:*LUC* under LL. Period length ± SD: **(C)** the wild type, 25.1 ± 1.3 h; *ELF4-OX*, 28.75 ± 0.95 h; **(D)** the wild type, 25.1 ± 1.3 h; *ELF3-OX*, 25.9 ± 1.6 h; *elf4-1 ELF3-OX*, 25.2 ± 0.9 h. Note that in *elf3-4* and *elf3-4 ELF4-OX* **(C)**, and in *elf4-1* **(D)**, *LHY*:*LUC* is nearly undetectable (arrow), but *elf4-1 ELF3-OX* regains *LHY*:*LUC* rhythms **(D)**. The wild type is the same in both panels. Error bars indicate SE, *n* = 24. cps, count per second. This experiment is representative of at least three independent replicates.

(E) Bioluminescence of *CCR2*:*LUC* under LL. Period length estimates: the wild type, 27.4 ± 0.9 h; *ELF3-OX*, 27.8 ± 1.1 h; *elf4-1 ELF3-OX*, 28.9 ± 0.8 h. Error bars indicate SE.

(F) Bioluminescence of *CCR2*:*LUC* in DD. Period length estimates: the wild type, 28.0 ± 1.3 h; *ELF3-OX*, 29.5 ± 1.7 h; *elf4-1 ELF3-OX*, 30.3 ± 1.4 h. Error bars indicate SE.

and ELF4 by in vitro pull-down experiments. For this, a recombinant ELF3M fragment fused at the N terminus to Maltose Binding Protein (MBP-ELF3M) was bound to amylose resin, and His_6-tagged ELF4 was applied. In the eluate fraction, we found both MBP-ELF3M and ELF4 (Figure 2C). Therefore, ELF3M mediates physical interaction with ELF4.

ELF4 Binding to ELF3 Is Crucial for ELF3 Nuclear Abundance

Observations that different domains of ELF3 are required for given protein interactions suggest that ELF3 could be functionally separated in its different domains. To examine this, we generated six different YFP-ELF3 fusion proteins, which directly corresponded to the ELF3 fragments used in the Y2H experiments (Figures 2A and 3A1), and analyzed their subcellular distribution in plant cells. For this, YFP-ELF3 fusions were expressed under the control of the 35S promoter in *Nicotiana benthamiana* epidermal cells (Voinnet et al., 2003). Consistent with previous studies (Liu et al., 2001; Yu et al., 2008), we found full-length ELF3 (YFP-ELF3F) localized in the nucleus where it formed distinct nuclear bodies (Figure 3A2). On the contrary, the N-terminal fragment of ELF3 (YFP-ELF3N) was nearly absent from the nucleus and accumulated preferentially in the cytoplasm (Figure 3A3). Furthermore, the middle domain (YFP-ELF3M) and a long N-terminal fragment (YFP-ELF3NM) were evenly distributed in the nuclear and cytoplasmic compartments (Figures 3A4 and 3A5). Finally, the C-terminal domain of ELF3 (ELF3C) was exclusively localized in few, but bright and large,

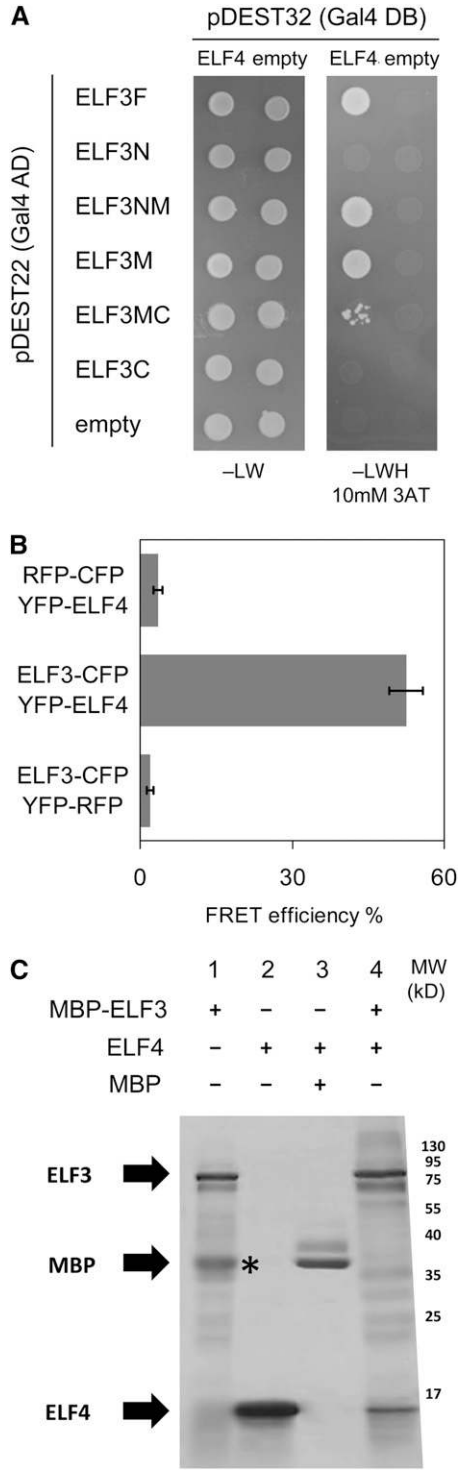

Figure 2. The Middle Domain of ELF3 Mediates the Physical Interaction with ELF4.

(A) The middle domain of ELF3 (ELF3M; residues 261 to 484) mediates the physical interaction with ELF4. Y2H assay of DB-ELF4 and ELF3-AD fragments. AD-ELF3 fragments are defined in Figure 3A. empty, AD or DB only; –LW and –LWH, dropout for Leu/Trp and Leu/Trp/His, respectively; 3AT, 3-amino-1,2,4-triazole. The Y2H experiments were performed three times with similar results.

(B) ELF3 and ELF4 interact in planta. FRET assay of ELF3-CFP and YFP-ELF4 in *N. benthamiana* (using the 35S promoter), $n = 10$. Error bars indicate SE. This experiment is representative of three independent replicates.

(C) ELF4 binds to the ELF3 middle domain (ELF3M) in vitro. SDS-PAGE gel: lane 1, fraction of His_6-MBP-ELF3M fragment eluted from the amylose column; lane 2, fraction of His_6-ELF4 eluted from the Ni-nitriloacetic acid column; lane 3, fraction of His_6-ELF4 fragment eluted from the amylose column (no ELF4 band, indicating lack of affinity for amylose); lane 4, ELF4 pulldown in the ELF3M:ELF3M-ELF4 fraction eluted from amylose resin, followed by size exclusion chromatography. Asterisk indicates contamination from proteolysis of MBP-ELF3M. MW, molecular weight.

nuclear structures (Figure 3A7). Consistently, the fragment comprising both the middle and C-terminal domains (ELF3MC) was preferentially nuclear (Figure 3A6). Thus, we found that the C-terminal domain of ELF3 is required for nuclear localization, which is in agreement with the prediction of a nuclear import signal in the C-terminal region of ELF3 (residues 591–600; Liu et al., 2001).

Next, we tested the effect of ELF4 on ELF3 cellular localization. For this, we coexpressed the YFP-ELF3M and YFP-ELF3NM fragments alone and with ELF4-CFP and tested if there was a change in the ELF3 cellular distribution. When expressed alone, ELF4-CFP showed a diffuse nuclear localization (Figure 3A8). We did not detect changes in the distribution for the YFP-ELF3 fusions that were already nuclear localized, which were ELF3F, ELF3MC, and ELF3C, nor for ELF3N, which was always found in the cytosol (data not shown). Interestingly, however, ELF3 coexpression with ELF4 dramatically increased the nuclear accumulation of both YFP-ELF3M and YFP-ELF3NM (Figures 3B1 and 3B2; see Supplemental Figure 2 online). Thus, ELF4 binding to the middle domain of ELF3 is crucial for nuclear abundance of ELF3, especially in the absence of the ELF3C domain.

ELF3 and ELF4 Colocalize in Nuclear Bodies

We have shown that ELF4 can increase ELF3 nuclear localization (Figure 3). In the nucleus, ELF4 distribution is diffuse, whereas ELF3 forms nuclear bodies (Figure 3; Yu et al., 2008). To investigate this further, we expressed full-length ELF3-YFP and ELF4-CFP fusion proteins under the control of their native promoters, ELF3pro:ELF3-YFP and ELF4pro:ELF4-CFP, in *N. benthamiana*. When expressed alone, we found that ELF3pro:ELF3-YFP (Figure 4A1) and ELF4pro:ELF4-CFP (Figure 4A2) were predominantly nuclear localized, although we observed cytoplasmic localization especially for ELF4pro:ELF4-CFP (Figure 4A2). In the nucleus, localization of both ELF3pro:ELF3-YFP and ELF4pro:ELF4-CFP was diffuse (Figures 4A1 and 4A2). When ELF3pro:ELF3-YFP and ELF4pro:ELF4-CFP were coexpressed, both localized in the nucleus (Figures 4B1 and 4B2), specifically in bright nuclear bodies, and the diffuse distribution of the fusion proteins was reduced (Figure 4C). Collectively, coexpression of ELF3pro:ELF3-YFP and ELF4pro:ELF4-CFP can alter the subnuclear distribution of both proteins, resulting in nuclear bodies.

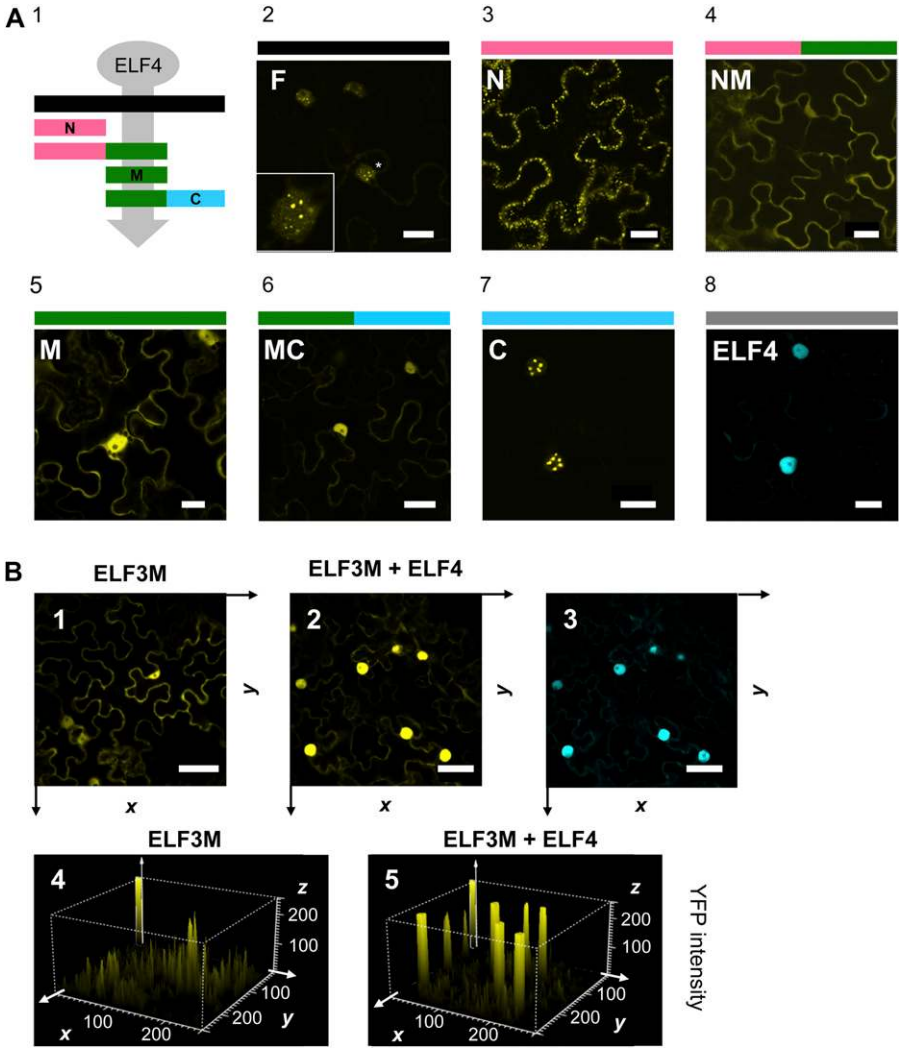

Figure 3. ELF4 Increases ELF3 Abundance in the Nucleus.

(A1) ELF3 fragments used for Y2H with the ELF3 AD (Figure 1) and for the ELF3 YFP constructs. The ELF4 arrow pointing to ELF3M represents the protein–protein interaction.
(A1) to **(A7)** Color bars: ELF3F (full length, black), ELF3N (residues 1 to 259, pink), ELF3M (residues 261 to 484, green), ELF3C (residues 485 to 695, blue), and ELF4 (full length, gray).
(A2) to **(A7)** YFP channel of epidermal cells of *N. benthamiana* infiltrated with YFP-ELF3 fragments. The color code refers to the scheme to the left. Bars = 20 μm.
(A2) YFP-ELF3F, magnification highlighted with an asterisk.
(A3) YFP-ELF3N is cytoplasmic.
(A4) and **(A5)** YFP-ELF3NM and YFP-ELF3M have both a cytoplasmic and nuclear distribution.
(A6) and **(A7)** YFP-ELF3MC and YFP-ELF3C are both localized in the nucleus.
(A8) CFP channel of epidermal cells of *N. benthamiana* infiltrated with ELF4-CFP. The photos are representative of three independent experiments.
(B1) to **(B5)** ELF4 increases ELF3M nuclear localization. Expression of YFP-ELF3M only: YFP channel **(B1)**. Coexpression of YFP-ELF3M and ELF4-CFP: YFP **(B2)** and CFP **(B3)** channel. Signal intensity of YFP channel: YFP-ELF3 alone **(B4)** from experiment in **(B1)**; coexpression of YFP-ELF3M and ELF4-CFP **(B5)** from the experiment in **(B2)**. The *z*, *x*, and *y* axes represent YFP intensity, horizontal plane, and vertical plane, respectively. Black arrows in **(B1)** and **(B2)** correspond to white arrows in **(B4)** and **(B5)**. This experiment is representative of three independent replicates.

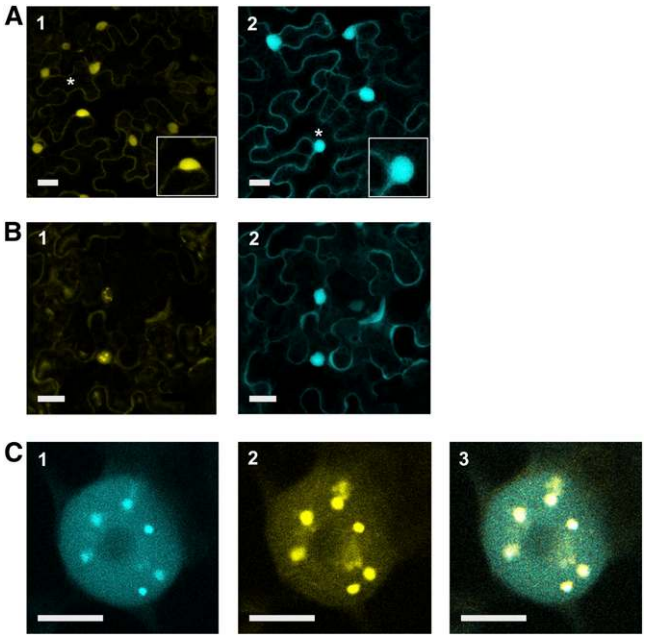

Figure 4. ELF3 Localizes in Nuclear Bodies in the Presence of ELF4.

Transient expression of ELF3 and ELF4 YFP/CFP fusion proteins in *N. benthamiana* epidermal cells.
(A1) and **(A2)** Individual expression of ELF3pro:ELF3-YFP (**[A1]**; YFP channel) and ELF4p:CFP-ELF4 (**[A2]**; CFP channel). The images represent the average of the 15-μm *z*-stack (10 slices). Asterisks indicate the nuclei magnified in bottom right corner in **(A1)** and **(A2)**. Bars = 20μm.
(B1) and **(B2)** Coexpression of ELF3pro:ELF3-YFP and ELF4pro:ELF4-CFP. YFP channel **(B1)**; CFP channel **(B2)**. The images represent the average of the 15-μm *z*-stack (10 slices). Bars = 20 μm.
(C1) to **(C3)** Nucleus where ELF3pro:ELF3-YFP and ELF4pro:ELF4-CFP are coexpressed. YFP channel **(C1)**, CFP channel **(C2)**, and merged YFP-CFP **(C3)**. Bars = 5 μm.

The ELF4 Recognition Site of ELF3 Is Required for Sustaining Circadian Period

To identify the ELF3 domain required for circadian function, we tested whether each of the YFP-ELF3 fragments described in Figure 3A could complement the *elf3-4* arrhythmic phenotype. These YFP-ELF3 fragments were expressed under the control of the 35S promoter. As expected, the subcellular localization of all the YFP-ELF3 fragments in stable *Arabidopsis* lines was similar to those in transiently transformed *N. benthamiana*. In particular, the localization of YFP-ELF3N was restricted to the cytoplasm (Figure 5, panel 2). Both YFP-ELF3NM and YFP-ELF3M fusion proteins were evenly distributed in the nucleus and cytoplasm (Figure 5, panels 3 and 4). By contrast, YFP-ELF3F and YFP-ELF3C localized in nuclear bodies (Figure 5, panels 1 and 7 and 6 and 9, respectively). In addition, diffuse nuclear localization was found for YFP-ELF3F and YFP-ELFMC fusion proteins (Figure 5, panels 1 and 7 and 5 and 8, respectively). Thus, the ELF3 fragments displayed similar subcellular localization in the stable transgenic lines (Figure 5) as in the transient experiments (Figure 3).

The complementation capacity of each YFP-ELF3 fusion protein to restore the *elf3-4* phenotype was tested using the *LHY:LUC* reporter. Consistent with the results in Figure 2, and with previous studies (Covington et al., 2001), the overexpression of YFP-ELF3 conferred a long circadian period of *LHY:LUC* under LL, when compared with the wild type (Figures 6A and 6C). Interestingly, the overexpression of YFP-ELF3MC was sufficient to reestablish circadian rhythms in *elf3-4*, albeit with a lower *LUC* activity, compared with YFP-ELF3 (Figures 6B and 6C). We did not obtain complementation of the *elf3-4* phenotype using overexpression of the other YFP-ELF3 fragments (see Supplemental Figure 3 online). Thus, both nuclear localization, conferred by the ELF3 C-terminal domain, and ELF4 binding mediated by the ELF3 middle domain are required for proper ELF3 circadian function.

ELF4 Is Localized Preferentially in the Nucleus in *Arabidopsis*

To confirm the subcellular localization of ELF4 in *Arabidopsis*, we generated YFP-ELF4-OX lines in the *elf4-1* background. Consistent with previous reports using transient assays (Figure 3; Khanna et al., 2003), we found that YFP-ELF4 localized diffusely

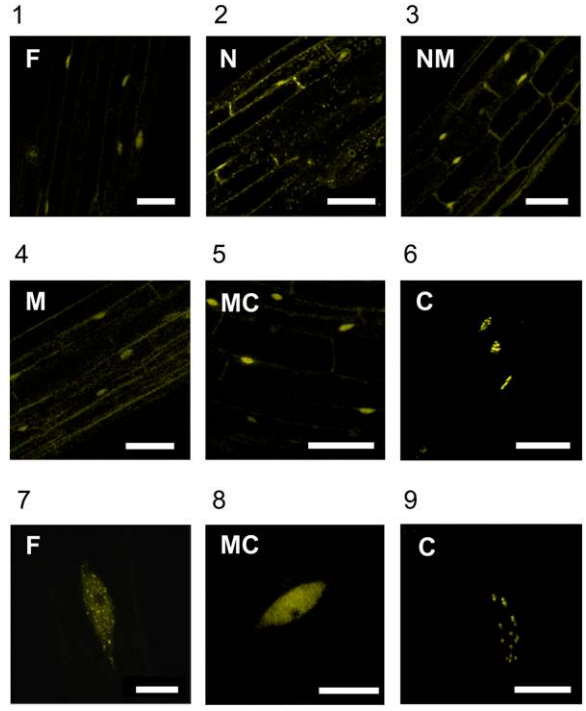

Figure 5. Subcellular Distribution of ELF3 in *Arabidopsis* Stable Transgenic Lines.

Confocal microscopy of *Arabidopsis* expressing YFP-ELF3 fragments (under the 35S promoter). (1) YFP-ELF3, (2) YFP-ELF3N, (3) YFP-ELF3NM, (4) YFP-ELF3M, (5) YFP-ELF3MC, (6) YFP-ELF3C, (7) YFP-ELF3F nuclei, (8) YFP-ELF3MC nuclei, and (9) YFP-ELF3C nuclei. Maximum projection of 6-μm stacks (1 to 6) and 4-μm stacks for nuclei (7 to 9). Bars = 50 μm in (1) to (6) and 10 μm in (7) to (9). The imaging was repeated two times with similar results.

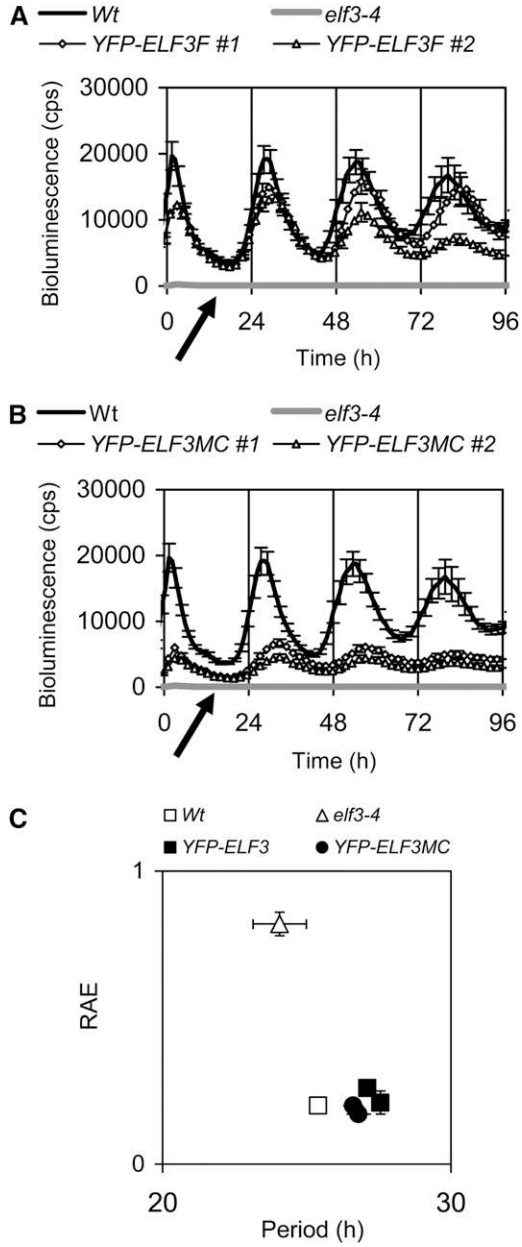

Figure 6. Defining a Functional Region of ELF3.

(A) to **(C)** Circadian rhythmicity of *LHY:LUC* under LL. Wild-type trace is the same in **(A)** and **(B)**. Two representative single-insertion lines for each of the YFP transgenes are shown (indicated by #1 and #2, respectively).

(A) YFP-ELF3 overexpression restores circadian oscillations and causes a lengthening of the period in the *elf3-4* background. Arrow indicates the low activity of *LHY:LUC* in *elf3-4*.

(B) YFP-ELF3MC overexpression restores *elf3-4* circadian oscillations and causes a lengthening of the period and low amplitude. Arrow indicates the *elf3-4* trace. Wild-type trace is the same in **(A)** and **(B)**. Error bars indicate SE, $n = 24$.

(C) Period versus relative amplitude error (RAE) of *LHY:LUC* under LL in **(A)** and **(B)**. Period and relative amplitude error estimates ± SE: the wild type, 25.4 ± 0.2 h/0.2 ± 0.01; *elf3-4*, 24.1 ± 0.9 h/0.82 ± 0.04; YFP-ELF3 #1, 27.6 ± 0.3 h/0.21 ± 0.04; YFP-ELF3 #2, 27.1 ± 0.3 h/0.26 ± 0.02; YFP-ELF3MC #1, 26.8 ± 0.4 h/0.17 ± 0.01; YFP-ELF3MC #2, 26.6 ± 0.3 h/0.2 ± 0.01.

in the nuclei of hypocotyl cells (Figure 7A). The YFP-ELF4 expression restored the arrhythmic *LHY:LUC* expression of *elf4-1* and conferred a long period with a similar rhythmicity to the wild type (Figures 7B and 7C), consistent with our previous observations of the *ELF4* overexpression effect (Figure 2C; McWatters et al., 2007).

ELF3/ELF4 Directly Represses *PRR9* Expression

Current mathematical models of the circadian clock do not explicitly include the roles of *ELF3* and *ELF4* (Zeilinger et al., 2006; Pokhilko et al., 2010). To describe mathematically a role for *ELF3* and *ELF4* in the circadian network, we constructed low-order linear time invariant (LTI) models of parts of the circadian system using a data set of clock gene expression data from LD and LL (Kolmos et al., 2011) as training data for the systems identification. A high fitness of an LTI model between two measured species meant that the model closely reproduced the data and revealed a strong probability that one of these species directly regulates the other. Some of the LTI models with high fitness described relationships between the clock components consistent with those known from previous experimental and modeling studies (Locke et al., 2006; Ding et al., 2007; Kolmos et al., 2009; Dalchau et al., 2010; Pokhilko et al., 2010), demonstrating that LTI models can describe key parts of the known circadian network (see Supplemental Data Set 1 online).

The LTI models predicted the positive arms of the clock, including *CCA1/LHY* to *PRR9* and *PRR7*, and *TOC1* to *CCA1/LHY*, and known negative feedback relationships of the central oscillator, which are *CCA1/LHY* to *TOC1*, and *PRR7* and *PRR9* to *LHY/CCA1* (Figure 8A). In addition to (re)identifying known connections within the circadian network, the LTI models revealed pathways currently not included in mathematical descriptions of the clock network. First, the LTI models predicted a link from the morning gene *LHY* to *ELF3/ELF4* (Figures 8B and 8C). Second, the LTI models predicted a pathway from *PRR9* to *GI* (Figure 8D; see Supplemental Data Set 1 online) but not from *PRR7* to *GI*, supporting the proposal that *PRR9* and *PRR7* function can be separated (Kolmos et al., 2009; Pokhilko et al., 2010). Finally, the LTI models predicted two regulatory links from *ELF3/ELF4* to *PRR9* and *PRR7* (Figures 8E and 8F).

As *PRR9* and *PRR7* expression in *elf4* (Kolmos et al., 2009) and *elf3* (Thines and Harmon, 2010; Dixon et al., 2011) is elevated, this implicates the *ELF3* and *ELF4* genes as direct genetic repressors of *PRR9* and *PRR7*. We thus tested if these *ELF* genes were sufficient to mediate repression, as predicted in the LTI models (Figures 8E and 8F). For this, we measured transcript accumulation of *PRR9* and *PRR7* in *ELF3-OX*, *ELF4-OX*, and *elf4-1 ELF3-OX* under LL and LD conditions. We found that both *ELF3-OX* and *ELF4-OX* alone are genetically sufficient to decrease transcript levels of *PRR9* under LL and LD (Figures 8G and 8I). For *PRR7*, we found a less pronounced decrease in its transcript accumulation than for *PRR9* under LL (Figure 8H). Under LD, *PRR7* levels in *ELF3-OX* and *ELF4-OX* were similar to the wild type (Figure 8J). Interestingly, for the *elf4-1 ELF3-OX* double mutant, we found similar levels of *PRR9* and *PRR7* as in *ELF3-OX* under LL (Figures 8G and 8H). This is consistent with *ELF3* being genetically downstream of *ELF4*, as shown in Figure

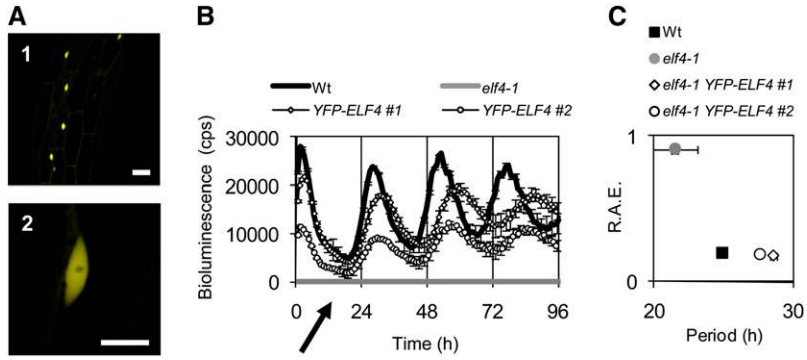

Figure 7. Subcellular Localization of ELF4 in *Arabidopsis* Stable Transgenic Lines.

(A) Confocal microscopy of hypocotyl cells from stable *Arabidopsis* lines expressing YFP-ELF4 under the 35S promoter in the *elf4-1* background. Bars = 25 μm in (1) and 10 μm in (2). The images are representative of at least two independent *elf4-1 YFP-ELF3-OX* lines (indicated as #1 and #2, respectively). The imaging was performed twice with similar results.

(B) Normalized bioluminescence of *LHY*:*LUC* under LL for the wild type (Wt), *elf4-1*, and *elf4-1 YFP-ELF4* lines. Arrow indicates the low activity of *LHY*:*LUC* in *elf4-1*. cps, counts per second.

(C) Period versus relative amplitude error (R.A.E.) plot of data from panel **(B)**.

Period and relative amplitude error values ± SE: the wild type, 24.93 ± 0.2 h/0.2 ± 0.01; *elf4-1*, 21.50 ± 0.17 h/0.91 ± 0.03; *elf4-1 YFP-ELF4 #1*, 28.63 ± 0.24 h/0.18 ± 0.01; *elf4-1 YFP-ELF4 #2*, 27.61 ± 0.19 h/0.19 ± 0.01. Error bars indicate SE, $n = 24$. This experiment was performed at least twice with similar results.

2. Under LD, *PRR9* expression was similarly reduced in *ELF3-OX* and *elf4-1 ELF3-OX* (Figure 8I). However, *PRR7* levels were increased in *elf4-1 ELF3-OX* when compared with *ELF3-OX* and to the wild type (Figure 8J). This does not necessarily mean that *ELF4* and *ELF3* are the only factors in this repression activity but provides validation to the LTI model predictions. Thus, the *ELF4-ELF3* signaling activity seems preferentially to repress *PRR9* but also acts at *PRR7*. This is consistent with our previous hypothesis of ELF4 action in the circadian network (Kolmos et al., 2009).

We then looked for phylogenetically conserved elements in the *PRR9* promoter that could directly mediate repression by an ELF4-ELF3 complex. For this, we used a shadowing approach and compared orthologous promoters of *Arabidopsis lyrata*, *Capsella rubella*, and *Arabis alpina* to that of *Arabidopsis*. This analysis revealed high conservation within the proximal *PRR9* promoter, an ~400-bp region that is crucial for the normal expression of *PRR9* (Conserved Region 1; Figure 9; see Supplemental Figure 4 online; Ito et al., 2005). Within Conserved Region 1, we found five fully conserved *cis*-elements: an evening element (EE; Harmer et al., 2000), a LUX binding site (LBS; Helfer et al., 2011), two G-boxes (Quail, 2000), and one morning element (Michael et al., 2008; Figure 9; see Supplemental Figure 4 online). Recently, it was reported that ELF3 could associate to the *PRR9* promoter (Dixon et al., 2011). We confirmed this result by a chromatin immunoprecipitation (ChIP) assay. We detected ELF3 association to the *PRR9* promoter and further delineated the binding site to a region that includes Conserved Region 1 (see Supplemental Figure 5 online). We did not find association of ELF3 to the *PRR7* promoter, consistent with the work of Dixon et al. (2011).

LUX Is Downstream of ELF4

Since *ELF3* does not obviously encode a DNA binding domain (Liu et al., 2001), it is likely that ELF3 association with the *PRR9* promoter requires a coupling component. As expression of numerous transcription factors modifies the circadian behavior of plants (Hazen et al., 2005; Hanano et al., 2008), multiple candidates exist. Interestingly, a recent publication found that the evening-expressed LUX (Helfer et al., 2011) can associate in vivo with the LBS, which we also defined as included in Conserved Region 1 of the *PRR9* promoter (Figure 9). Thus, we hypothesized that *LUX* could be a component of the *ELF3*/*ELF4* repressive activity. To test this, we created double mutants that overexpressed *YFP-LUX* fusions (*LUX-OX*) in the *elf3-4* and *elf4-1* backgrounds, respectively. Since LUX is a transcription factor, nuclear localization was expected. Hence, we also tested the subcellular distribution of LUX in these lines. YFP-LUX localized diffusely in the nucleus regardless of the genetic presence of *ELF3* or *ELF4* (Figure 10). Then, we tested if *LUX-OX* could restore the *elf3* and *elf4 LHY*:*LUC* phenotypes, respectively (Figures 11B to 11D). In the context of wild-type *ELF3* and *ELF4*, and consistent with previous reports (Onai and Ishiura, 2005; Helfer et al., 2011), we found that *LHY*:*LUC* expression in the *LUX-OX* background was rhythmic under LL but that the oscillations gradually faded (Figures 11A to 11D). Interestingly, just like *ELF3-OX* suppressed the *elf4-1* phenotype (Figure 1D), the *elf4-1 LUX-OX* double mutant resulted in overt *LHY*:*LUC* rhythmicity (Figures 11B and 11D). Furthermore, *LUX-OX* was ineffective at complementing *elf3-4* (Figures 11C and 11D). Taken together, *LUX* is a downstream component of *ELF4* signaling that requires *ELF3* action.

DISCUSSION

ELF3 and ELF4 play pivotal roles in the circadian clock mechanism and in the integration of light signals to the clock (McWatters et al., 2000; Covington et al., 2001; Thines and

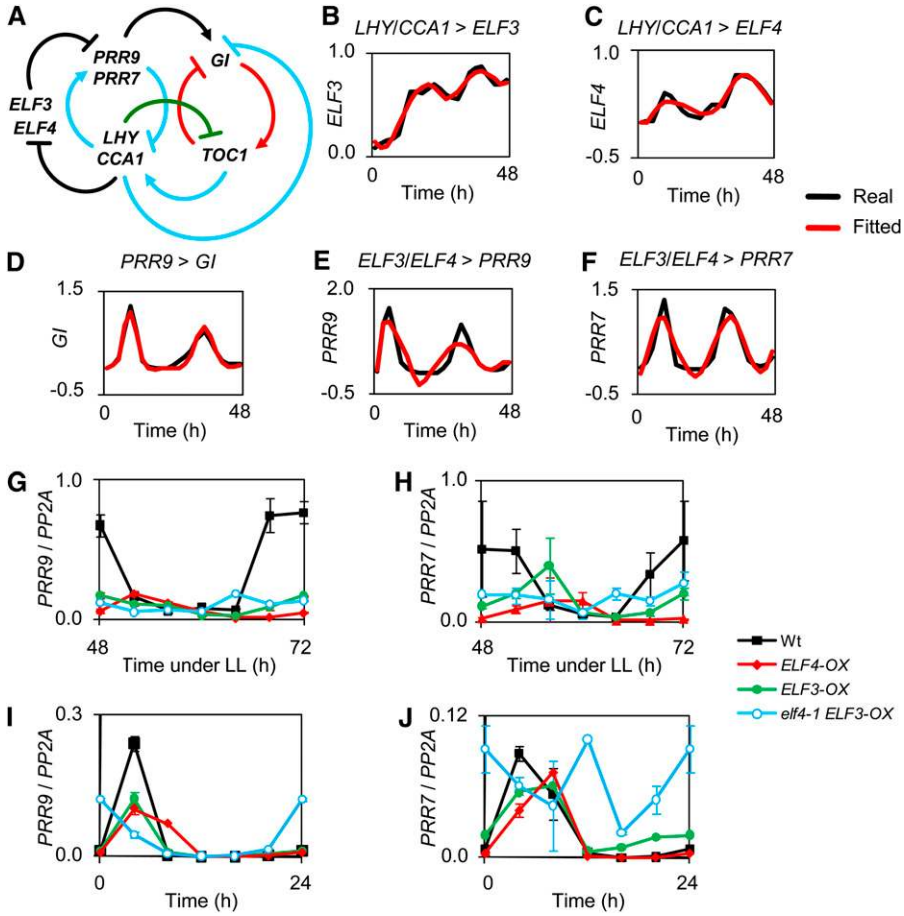

Figure 8. LTI Modeling Includes ELF3/ELF4 in the Circadian Network.

(A) Expanded circadian clock model incorporates *ELF3* and *ELF4*. LTI models of the circadian system using a data set of clock gene expression data from LD and LL (Kolmos et al., 2011) as training data for the systems identification. Newly described links are in black. Links common between the three-loop model (Locke et al., 2006) and our model are blue (>60% fitness) and green (50 to 60% fitness). Links existing in the three-loop model, but not in our model, are in red.

(B) to **(F)** Fitness of LTI models to real expression data. Real (black) and simulated (red) data curves of gene expression: *LHY/CCA1* links to *ELF3* **(B)**, *LHY/CCA1* links to *ELF4* **(C)**, *PRR9* links to *GI* **(D)**, *ELF3/ELF4* links to *PRR9* **(E)**, and *ELF3/ELF4* links to *PRR7* **(F)**.

(G) and **(H)** *PRR9* **(G)** and *PRR7* **(H)** transcript accumulation under LL in the wild type, *ELF3-OX*, *ELF4-OX*, and *elf4-1 ELF3-OX*. Samples were collected after 48 h under LL. Expression values are normalized to *PP2A* and are representative of two biological replicates.

(I) and **(J)** *PRR9* **(I)** and *PRR7* **(J)** transcript accumulation under LD (short days, 8 h light/16 dark) in the wild type, *ELF3-OX*, *ELF4-OX*, and *elf4-1 ELF3-OX*. Expression values are normalized to *PP2A* and are representative of two biological replicates. Wt, wild type.

Harmon, 2010; Dixon et al., 2011). However, the molecular basis of ELF3 and ELF4 action is poorly understood. We found *ELF3* to be genetically downstream of *ELF4* (Figure 1), and consistent with previous hypotheses (Kikis et al., 2005; Kolmos and Davis, 2007; Kolmos et al., 2009), *elf3* and *elf4* displayed arrhythmic and low expression of *CCA1*:*LUC*. This phenotype was more severe in the *elf3* and *elf3 elf4* mutants than in *elf4*. The overexpression of *ELF3* (*ELF3-OX*) conferred long period of *LHY*:*LUC*, as does overexpression of *ELF4* (*ELF4-OX*; Figures 1C and 1D), supporting the role of the *ELF* genes as decelerators of circadian speed (Covington et al., 2001; Thines and Harmon, 2010; Kolmos et al., 2011). Interestingly, we found that *ELF3-OX* restored rhythmicity of *elf4* for both morning (*LHY*:*LUC*) and evening (*CCR2*:*LUC*) expressed reporters (Figures 1D to 1F). Thus, *ELF3* is epistatic to *ELF4*.

ELF3 is a multifunctional protein that has different interaction domains to bind both clock- and light-signaling components (Liu et al., 2001; Yu et al., 2008). We found that the middle domain of ELF3 (ELF3M, residues 261 to 484) mediated interaction with ELF4 (Figures 2 and 3). Previous reports showed that this middle domain also mediates the ELF3–GI interaction (Yu et al., 2008), whereas the N terminus of ELF3 is required for both phyB and CONSTITUTIVELY PHOTOMORPHOGENIC1 (COP1) binding (Liu et al., 2001; Yu et al., 2008). In addition, the different YFP-ELF3 fusion proteins (Figure 3A) were found to have different subcellular localizations both in a transient assay (Figure 3) and in

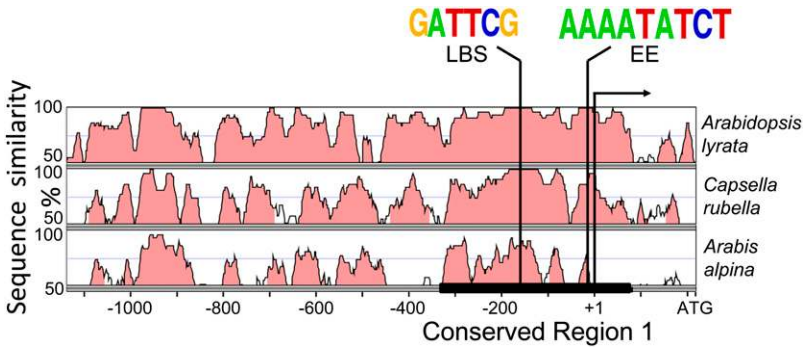

Figure 9. Phylogenetically Conserved Region of the *PRR9* Promoter.

Pairwise alignments of the *A. thaliana PRR9* promoter to orthologous sequences of *A. lyrata*, *C. rubella*, and *A. alpina*, respectively, shown as VISTA plots. Light-red color indicates regions where a sliding window of at least 30 bp has >70% identity. Conserved Region 1 (−331 to +89) is highlighted with a black line. Vertical bars indicate the position of highly conserved LBS, EE, and the translational initiation codon (arrow). Conservation of LBS and EE is shown as WEBLOGO.

stable transgenic lines (Figure 5). Full-length YFP-ELF3 was predominantly nuclear and formed distinct nuclear bodies, consistent with previous reports (Liu et al., 2001; Yu et al., 2008). The C-terminal domain of ELF3 seems to mediate nuclear localization since YFP-ELF3C localized exclusively in distinct nuclear bodies (Figures 3 and 5). This is consistent with a putative nuclear localization signal within this fragment (Liu et al., 2001). Both the ELF3NM and ELF3M fragments were distributed in the nucleus as well as in the cytoplasm (Figures 3 and 5), suggesting that the ELF3M domain, which mediates ELF4 interaction (Figure 2), also confers nuclear localization. When ELF3NM and ELF3M fragments were coexpressed with ELF4, we found a dramatic nuclear redistribution (Figure 3B; see Supplemental Figure 2 online). Since ELF4 was preferentially nuclear (Figures 3 and 7), our results are consistent with ELF4 acting to increase the nuclear pool of ELF3. Analogous mechanisms of cytoplasmic-to-nuclear distribution dynamics are found in several circadian systems (Herrero and Davis, 2012). In plants, PRR5 was reported to stabilize the TOC1 nuclear pool (Wang et al., 2010). In mice and flies, the CLOCK nuclear pool is maintained by the interaction with BMAL and CYCLE, respectively (Kondratov et al., 2003; Hung et al., 2009). Thus, ELF4 association to ELF3 functions to restrict it to the nucleus, and this is the likely activation step to initiate ELF3 repressive action on the clock.

Both clock- and light-signaling components localize in nuclear bodies (Más et al., 2000; Chen, 2008; Yu et al., 2008; Wang et al., 2010; Herrero and Davis, 2012). For ELF3, we found that the C termini were required for nuclear bodies (Figures 2 and 4). Notably, the nuclear bodies observed for full-length YFP-ELF3 were different in size and number to the ones observed for YFP-ELFC (Figures 2 and 4). We found that YFP-ELF3 full-length nuclear bodies were small and numerous and these bodies resembled the nuclear foci where ELF3, COP1, and GI colocalized (Yu et al., 2008). In addition, the YFP-ELF3 bodies resembled the phyB nuclear bodies observed for phyB-green fluorescent protein (GFP) (Oka et al., 2008). Nuclear foci containing phyB and COP1 have been associated with proteasome-mediated degradation (Chen, 2008; Yu et al., 2008; Chen et al., 2010). On the contrary, we found that ELF3C nuclear bodies were large and less numerous compared with full-length ELF3 (Figures 2 and 4). In *N. benthamiana*, the ELF3C bodies were similar in size and shape to the ones observed for the TOC1–PRR5 interaction (Wang et al., 2010; both experiments used a similar experimental setup). Notably, the TOC1-PRR5 foci were only seen following coexpression (Wang et al., 2010). Similarly, we observed colocalization of ELF3pro:ELF3-YFP and ELF4pro:ELF4-CFP in bright nuclear bodies when they were coexpressed (Figure 4). These results suggest that ELF3 can localize into two different subnuclear compartments: (1) The interaction of ELF3 with phyB and COP1 through the ELF3N domain (Liu et al., 2001; Yu et al., 2008) targets ELF3 to numerous small nuclear bodies, and (2) the ELF3C domain, and the ELF3M domain through ELF4 interaction, targets ELF3 to few but large nuclear bodies.

The molecular basis of ELF3 action has continued to be vague. We found that the ELF3 protein displays a modular structure. Both the ELF4 binding (ELF3M) and the nuclear-targeting (ELF3C) domains were required for complementation of *elf3-4* arrhythmicity (Figure 6). Interestingly, we determined that the N-terminal domain of ELF3 was dispensable for ELF3 circadian function, and alone, preferentially localized in a cytoplasmic pool (Figures 3 and 5). Notably, this N-terminal domain mediates physical interaction of ELF3 with the E3-ligase COP1 (Yu et al., 2008) and the phyB photoreceptor (Liu et al., 2001). COP1 was reported to target ELF3 for degradation by the proteasome (Yu et al., 2008). ELF3 and phyB have opposite roles in controlling circadian periodicity. *ELF3-OX* and the *phyB* mutant display respective long-periodicity phenotypes (Devlin and Kay, 2000; Covington et al., 2001). *PHYB-OX* and the reduced function allele *elf3-12* display short periodicity (Kolmos et al., 2011). In addition, the short-period phenotype of *elf3-12* was enhanced by *PHYB-OX* (Kolmos et al., 2011). As a result, we propose that COP1 and phyB interactions negatively modulate ELF3 activity. Furthermore, as ELF4 activity in the dark mediates the correct timing of *PRR9* expression (Kolmos et al., 2009), this could suggest that ELF4 binding to ELF3 counteracts both COP1- and phyB-mediated repression of ELF3. This could account for the arrhythmicity

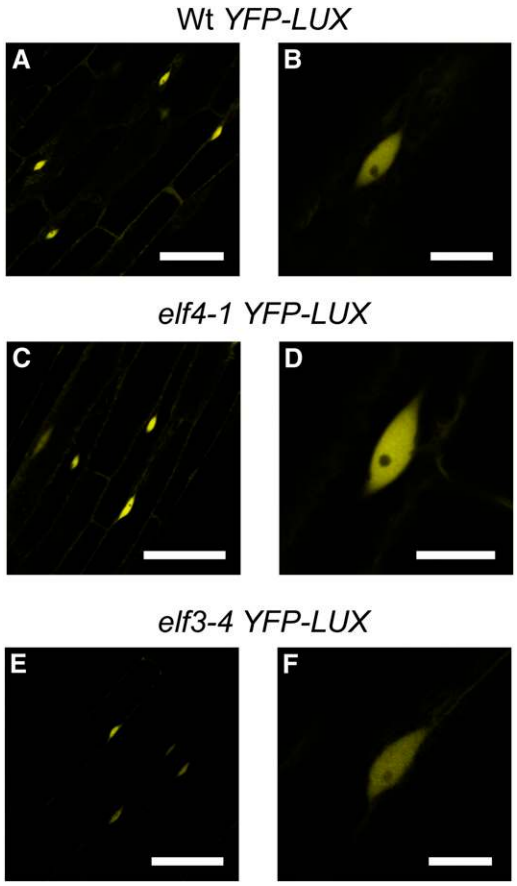

Figure 10. LUX Nuclear Localization Is Independent of ELF4 and ELF3.

YFP-LUX nuclear localization is not affected in the *elf4-1* and *elf3-4* backgrounds. YFP confocal microscopy of hypocotyl epidermal cells from *Arabidopsis* YFP-LUX lines. The wild type (**[A]** and **[B]**), *elf4-1* (**[C]** and **[D]**), and *elf3-4* (**[E]** and **[F]**). Bars = 50 μm in **(A)**, **(C)**, and **(E)** and 10 μm in **(B)**, **(D)**, and **(F)**. The images are representative of two independent lines per background. The experiments were performed twice with similar results.

observed in *elf4*. Taken together, the role of ELF3 to sustain circadian oscillations requires both interaction with ELF4 and nuclear localization, whereas association with phyB and COP1 may not be required for such sustaining action of ELF3.

We were able to model parts of the circadian network using LTI models. These LTI models predicted many known connections of the circadian network (Figure 8A), such as the central loop (*LHY*/*CCA1* and *TOC1*) and the morning loop (*LHY*/*CCA1* and *PRR7*/*PRR9*) and also previously unidentified connections involving *ELF3* and *ELF4* (Figure 8A), which we subsequently verified by experimentation. The connection between *LHY*/*CCA1* and *ELF4* is consistent with recent findings that *CCA1* acts as a transcriptional repressor by associating to the *ELF4* promoter (Li et al., 2011) and the *ELF3* promoter (Lu et al., 2012). Moreover, the LTI models connected *ELF3*/*ELF4* to *PRR7* and *PRR9*. In both *ELF3-OX* and *ELF4-OX*, the transcript accumulation of *PRR9*, and to a lesser extent *PRR7*, was decreased when compared with the wild type (Figures 8G to 8J). This is consistent with ELF3 and ELF4 working together (Figures 2 and 3) in a corepressor complex that can physically associate to the *PRR9* promoter (see Supplemental Figure 5 online). Nusinow et al. (2011) recently identified the evening complex (EC), a corepressor consisting of ELF4, ELF3, and LUX crucial to the transcriptional regulation of *PHYTOCHROME INTERACTING FACTOR4* (*PIF4*)/*PIF5* rhythmic expression and diurnal growth. Hence, it is possible that ELF3 and ELF4 indirectly promote *LHY* and *CCA1* expression by repressing *PRR9* and *PRR7*, consistent with low levels of *LHY* and *CCA1* found in *elf3* and *elf4* mutants (Kikis et al., 2005; McWatters et al., 2007; Dixon et al., 2011; Kolmos et al., 2011).

Some known connections of the circadian system could not be modeled using low-order LTI models, notably the activating link from *GI* to *TOC1* and the repressive links from *CCA1*/*LHY* to *GI* (Figure 8). The failure of LTI models to fit the data for these connections suggests that it is not possible to approximate these two relationships with linear functions. This could mean that the *GI*-to-*TOC1* and *CCA1*/*LHY*-to-*GI* connections bare fundamental nonlinearities in their systems, unlike the other connections in the oscillator that can be approximated with linear models. In the mass-action models of Millar and coworkers (Locke et al., 2006; Pokhilko et al., 2010), these two relationships are nonlinear, involving sigmoidal functions. Thus, computational analysis using mass-action kinetics or systems identification of LTI models, both identify these two connections as major nonlinear steps in the circadian progression. Nonlinearities are essential for sustained oscillations in constant conditions, and it is possible that *GI*(*Y*)-to-*TOC1* and *CCA1*/*LHY*-to-*GI*(*Y*) could be the steps critical for sustained oscillations.

ELF3, ELF4, and LUX have each been reported to associate to the *PRR9* promoter (Dixon et al., 2011; Helfer et al., 2011). Moreover, LUX and ELF3 associate to the same evolutionarily conserved region (Conserved Region 1; Figure 9) within the *PRR9* promoter (Helfer et al., 2011; see Supplemental Figure 5 online). Interestingly, we found that similar to *ELF3-OX*, overexpression of *LUX* could restore *elf4* arrhythmicity. As LUX appears to be nuclear localized regardless of the presence of ELF4 and ELF3 (Figures 10C to 10F), the cooperative repression of ELF3/ELF4 and LUX seems to be required for sustained circadian rhythmicity. This cooperation is consistent with their similar defects in clock-controlled gene expression and physiological phenotypes observed in their corresponding null alleles (Covington et al., 2001; Doyle et al., 2002; Hazen et al., 2005; Kikis et al., 2005; Onai and Ishiura, 2005; McWatters et al., 2007; Kolmos et al., 2009). We note here that for the EC, LUX is required for DNA association and ELF3 for complex formation (Nusinow et al., 2011). This is in agreement with our observations that both LUX and ELF3 overexpression restored *elf4* arrhythmicity (Figures 1 and 11). Furthermore, we found that ELF4 increased ELF3 nuclear distribution and localization in nuclear bodies (Figures 3 and 4). This is consistent with the reported low levels of ELF3 in the *elf4* mutant (Nusinow et al., 2011). Hence, we hypothesize that the subcellular distribution of ELF3 could be a mechanism to modulate the repressive activity of the EC.

It was reported that a *PRR9* promoter fragment containing only the EE was insufficient in sustaining *PRR9* rhythmic expression under free-running conditions. A larger promoter fraction (−172

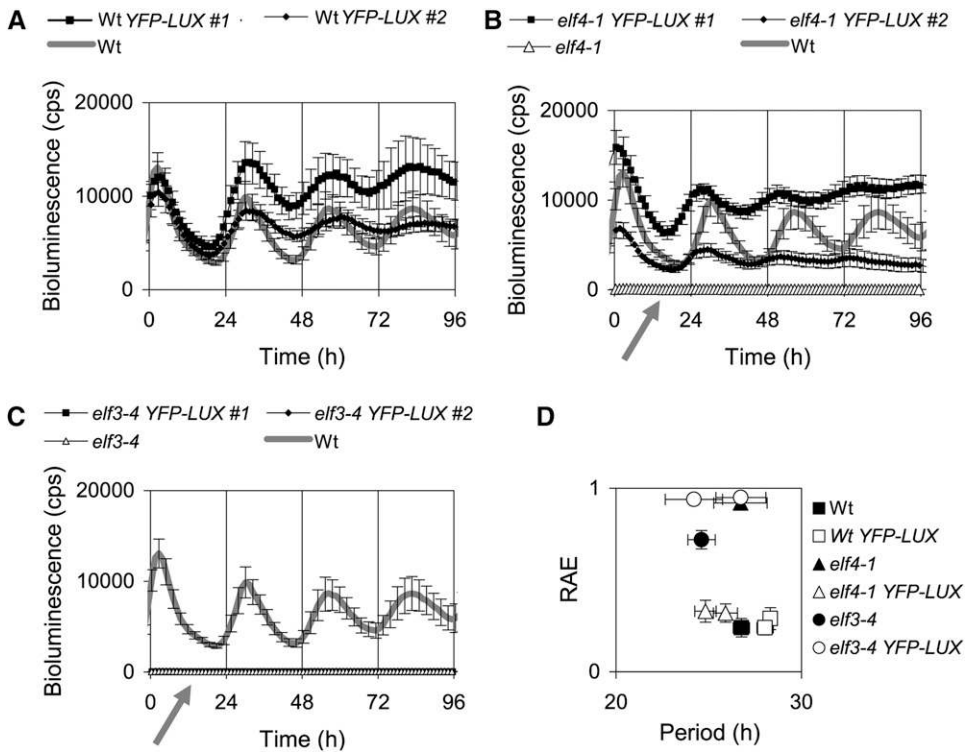

Figure 11. *LUX* Is Downstream of *ELF4* Action.

(A) to **(C)** *LHY*:*LUC* rhythms under LL of YFP-LUX in the wild type **(A)**, *elf4-1* **(B)**, and *elf3-4* **(C)** background, respectively. Two representative single-insertion lines for each of the YFP transgenes are shown (indicated by #1 and #2). Error bars indicate SE, $n = 24$. Arrows indicate low levels of *LHY*:*LUC* in *elf4-1* **(B)** and *elf3-4* **(C)**.

(D) Period versus relative amplitude error (RAE) of *LHY*:*LUC* rhythms from data in **(A)** to **(C)**. Period length/relative amplitude error ± SE: the wild type, 27.7 ± 0.4 h/0.28 ± 0.05; *elf3-4*, 23.7 ± 3.9 h/0.94 ± 0.03; *elf4-1*, 27.9 ± 2.8 h/0.96 ± 0.03; wild-type *YFP-LUX #1*, 26.8 ± 0.8 h/0.36 ± 0.04; wild-type *YFP-LUX #2*, 27.3 ± 1.1 h/0.35 ± 0.05; *elf3-4 YFP-LUX #1*, 24.2 ± 3.1 h/0.96 ± 0.02; *elf3-4 YFP-LUX #2*, 28.5 ± 2.6 h/0.93 ± 0.03; *elf4-1 YFP-LUX #1*, 26.3 ± 0.7 h/0.38 ± 0.04; *elf4-1 YFP-LUX #2*, 26.4 ± 0.6 h/0.32 ± 0.05.

bp to +225) including Conserved Region 1, which contains both the EE and the LBS, was shown to be required for circadian regulation of *PRR9* expression (Ito et al., 2005; Helfer et al., 2011). Hence, both transcriptional repression mediated cooperatively by ELF3/ELF4 and LUX and transcriptional activation mediated by CCA1 are required for rhythmic expression of *PRR9*. The competition between activator and repressor complexes has been found to be critical for sustaining circadian oscillations in plants (Li et al., 2011; Herrero and Davis, 2012) and in other clock systems, such as in mice and flies (Matsumoto et al., 2007; Ukai-Tadenuma et al., 2008; Ukai-Tadenuma et al., 2011). Therefore, it is plausible that competition of coactivators and corepressors at the promoters of clock-controlled genes is generally important for circadian oscillator function in eukaryotic organisms.

METHODS

Plant Materials

All the *Arabidopsis thaliana* lines used in this study are in the Wassilewskija-2 background and are listed in Supplemental Table 1 online. Stable transgenic lines were obtained via *Agrobacterium tumefaciens*–mediated transformation using a modified floral dip method (Davis et al., 2009). For YFP and CFP constructs, T1 plants were selected in Murashige and Skoog 1-containing agar plates supplemented with phosphinothricin. T2 lines were selected based on phosphinothricin resistance, hypocotyl segregation, circadian phenotype, and confocal laser microscopy analysis. For all experiments in this study, selected T3 lines homozygous for the corresponding T-DNA insertion were used. The bioluminescence assays were all performed as described by Kolmos et al. (2009). For LL conditions, 9μmol blue light and 7μmol red light intensities were used.

Cloning of *ELF3*, *ELF4*, and *LUX* Fragments

The ELF3-derived fragments, ELF4 and LUX, were amplified from cDNA. For the YFP-ELF3 and ELF3-CFP constructs, Wassilewskija genomic DNA was used as template. PCR amplification was performed with PfuUltra II Fusion HS DNA polymerase and subcloning performed with Gateway pDONR201 (Invitrogen). The primers are listed in Supplemental Table 2 online. For Y2H, the corresponding inserts were shuttled from pDONR201 to pDEST22 (Gal4 AD) and pDEST32 (Gal4 DB) (Invitrogen). The plant binary Gateway expression vectors pENSG-YFP-X and pENSG-X-CFP were used to obtain full-length *35S*:*YFP-ELF3*, *35S*:*YFP-ELF3* fragments, *35S*:*YFP-LUX*, and *35S*:*ELF4-CFP*.

Cloning of ELF3:ELF3-YFP and ELF4:ELF4-CFP

The Gateway cassette of pDESTR4R3 (Invitrogen) was inserted into the binary vector pPZP211 (Hajdukiewicz et al., 1994) to obtain pPZP211R4R3. The inserts were amplified by PCR (see Supplemental Table 2 online) and cloned as follows. The *ELF3* promoter (3 kb upstream of the 5′ untranslated region) and the *ELF4* promoter (Doyle et al., 2002) were cloned in pDONRP4-P1R (Invitrogen). The *ELF3* genomic coding region (including 3′ untranslated region) and the *ELF4* coding region were cloned in pDONR201. The CFP and YFP cDNAs were cloned in pDONRP2R-P3 (Invitrogen). The three different pDONR constructs were recombined with pPZP211R4R3 by Multi-Gateway LR reaction (Invitrogen) to obtain ELF3pro:ELF3-YFP and ELF4pro:ELF4-CFP. The final plasmids were introduced into *Agrobacterium* strain GV3101.

Y2H Experiments

The recombinant pDEST22 (Gal4 AD) and pDEST32 (Gal4 DB) vectors were cotransformed into *Saccharomyces cerevisiae* AH109 strain by Li-Ac Small Scale Transformation following Clontech's protocol. Y2H experiments were performed using minimal SD base (Clontech) with –His/–Leu/–Trp DO supplement amino acid dropout (Clontech) and supplemented with 3-amino-1,2,4-triazole (1 to 10 mM) to test the strength of the interaction.

FRET and Microscopy

Transient *Agrobacterium*-mediated expression in *Nicotiana benthamiana* was performed as described by Voinnet et al. (2003). After agroinfiltration, plants were kept in the greenhouse for 3 d (long days) before microscopy imaging or protein extraction. Seven-day-old plants grown under LD (12 h light/12 h dark) were used for imaging of *Arabidopsis* transgenic lines.

For all experiments, the Leica TCS SP2 AOBS confocal laser scanning microscope with an HCX PL APO CS 40.0x1.25 oil UV objective and Leica Confocal Software (Leica Microsystems) were used. *N. benthamiana* leaf excisions and *Arabidopsis* seedlings were submerged in water. The spectral settings were as follows: for YFP, excitation of 514 nm and emission of 518 to 570 nm; for CFP, excitation of 405 nm and emission spectra of 460 to 550 nm. Pinhole was set to airy 1 (optimal for objective). Laser intensity was ~40%. For each image channel, voltage and offset were adjusted to obtain a linear look-up table of fluorescence intensity. For individual information regarding microscopy images, see the Supplemental Data Set 2 online.

FRET efficiency was assayed by acceptor photobleaching. The spectral settings before and after bleaching were as follows: CFP (donor), excitation of 405 nm and emission of 450 to 505 nm; YFP (acceptor), excitation of 514 nm and emission of 518 to 590 nm. Laser intensity was 40%. For bleaching, 100% intensity of 405 nm was applied until YFP levels were reduced to ~25%. Then, FRET efficiency was calculated with the following formula: FRET efficiency = CFP intensity postbleaching – CFP intensity prebleaching/CFP intensity postbleaching.

In Vitro Pull-Down Assays

The *ELF3* middle fragment (encoding residues 251 to 520) was cloned into His_6-MBP–tagged pET28a+ vector, resulting in His_6-MBP-ELF3M. The His_6-MBP construct was prepared by introducing MBP into pET28a+. The vector pET28a-ELF4, resulting in His_6-ELF4, was described (Kolmos et al., 2009). All plasmids were introduced into the *Escherichia coli* expression strain Rosetta(DE3)pLysS. For in vitro pull-down assays, MBP-His_6-ELF3M and His_6-ELF4 recombinant proteins were initially purified using Ni-nitriloacetic acid columns. Binding buffers used were as follows: for ELF3M protein, 20 mM Tris-HCl, pH 7.8, 200 mM NaCl, and 1 mM EDTA; for ELF4 protein, 20 mM Tris-HCl, pH 7.8, 500 mM NaCl, and 1 mM EDTA. The proteins were purified using a stepwise gradient of imidazole in the buffer. His-tag affinity purification was followed by desalting to remove high salt and imidazole. Next, His_6-MBP-ELF3M eluted in low-salt buffer was passed through an amylose resin column for MBP-affinity chromatography. The column was washed first with 20 mM Tris-HCl, pH 7.5, and 1 mM EDTA and next with 20 mM Tris-HCl, pH 7.5, 70 mM NaCl, and 1 mM EDTA. Subsequently, purified His_6-ELF4 was passed through the His_6-MBP-ELF3M bound amylose column. The washing was repeated as previously described. Finally, the bound His_6-MBP-ELF3M protein was eluted using elution buffer (20 mM Tris-HCl, pH 7.5, 70 mM NaCl, and 1 mM EDTA). This was followed by size exclusion chromatography. Controls (only His_6-MBP-ELF3M or only His_6-ELF4) were run in parallel during the second step of the affinity chromatography. Eluted fractions were resolved on an SDS-PAGE gel, Coomassie Brilliant Blue stained, and imaged. The recombinant proteins were identified by mass spectrometry as maintaining fidelity.

Mathematical Modeling

A detailed description of mathematical modeling methods is available in Supplemental Data Set 1 online and used RNA expression data from Kolmos et al. (2011). This is provided as Supplemental Data Sets 3 and 4 online.

Phylogenetic Shadowing

Sequences from *Arabidopsis*, *A. thaliana* and *Arabidopsis lyrata*, were obtained from The Arabidopsis Information Resource (www.Arabidopsis.org). The *Capsella rubella* sequence was assembled from raw sequence reads (http://trace.ncbi.nlm.nih.gov/Traces/sra/sra.cgi). The *Arabis alpina* sequence was obtained from our internal genome-sequencing project. Pairwise alignments were performed using Shuffle LAGAN (Brudno et al., 2003). VISTA plots were made with the VISTA browser (Mayor et al., 2000), with a calculation window of 30 bp and a consensus identity of 70%. Multiple sequence alignments were performed with DIALIGN (Morgenstern, 2004). Conserved *cis*-regulatory elements were visualized with WEBLOGO (Crooks et al., 2004).

Quantitative PCR and ChIP

ChIP experiments were basically performed as described by Perales and Más (2007). Commercial anti-GFP antibody (Roche) in 1/100 dilution was used for immunoprecipitation. Primers used for amplification of *PRR9* and *PRR7* promoters are listed in Supplemental Table 3 online. All primers were designed using Primer3Plus (Untergasser et al., 2007) to obtain amplicon sizes of 150 to 200 bp. Primer efficiencies were calculated for melting temperature of 58°C. Quantitative PCR (qPCR) was done with IQ SYBR Green Supermix (Bio-Rad) in the iCycler iQ5 Multicolor real-time PCR detection system (Bio-Rad). Expression values of ChIP samples were normalized to expression values of input samples to calculate the percent of enrichment. Additional negative control of ChIP without anti-GFP gave similar values as the *elf3-4* nontransgenic line ChIP with anti-GFP.

RNA extraction for expression analysis of *PRR9* and *PRR7* was performed on ~7-d-old seedlings at the time points indicated. Growth conditions, qRT-PCR, and primer sequences were previously described (Kolmos et al., 2009). Primer efficiencies were determined for an annealing temperature of 58°C. The qRT-PCR was analyzed with the Bio-Rad software package version 2.0 according to the manufacturer's recommendations. The reference gene for qPCR was *PROTEIN PHOSPHATASE2a* subunit A3 (*PP2A*; At1g13320); forward, 5′-TATCGGATGACGATTCTTCGTGCAG-3′; reverse, 5′-GCTTGGTCGACTATCGGAATGAGAG-3′. Gene expression is shown as the average of three technical replicates, and error bars represent SD among the technical replicates. The results presented are representative of at least two biological replicates.

Accession Numbers

Sequence data of *PRR9* promoters in this article can be found in the Arabidopsis Genome Initiative and GenBank/EMBL databases under the following accession numbers: JF293082 (*A. thaliana*); JF293083 (*A. lyrata*); JF293084 (*C. rubella*); and JF293085 (*A. alpina*) as the population study data set under the accession number 332015065.

Supplemental Data

The following materials are available in the online version of this article.

Supplemental Figure 1. Genetic Epistasis of *ELF3* to *ELF4*.

Supplemental Figure 2. Coexpression of YFP-ELF3 Fragments with ELF4.

Supplemental Figure 3. Complementation Test of *elf3-4* with YFP-ELF3 Fragments.

Supplemental Figure 4. Evolutionarily Conserved *cis*-Elements of the *PRR9* Promoter.

Supplemental Figure 5. ELF3 Associates to Conserved Region 1 in the *PRR9* Promoter.

Supplemental Table 1. *Arabidopsis* Transgenic Lines.

Supplemental Table 2. Primers Used for Molecular Cloning.

Supplemental Table 3. Primers Used for Amplification of *PRR9* and *PRR7* Promoters in ChIP.

Supplemental Data Set 1. Mathematical Modeling.

Supplemental Data Set 2. Microscopy File.

Supplemental Data Set 3. LD Data Set.

Supplemental Data Set 4. LL Data Set.

ACKNOWLEDGMENTS

We thank Amanda M. Davis for technical assistance, Chiarina Darrah for the modified pPZP221 vector, and Paloma Más for training on the ChIP assay. S.J.D. received funding from the Max-Planck-Gesellschaft and Deutsche Forschungsgemeinschaft (DA 1061/4-1; SPP 1530/1).

AUTHOR CONTRIBUTIONS

S.J.D., G.C., M.J., A.W., and J.G. conceived the project. E.H., E.K., N.B., Y.Y., M.W., M.C.B., H.U., and R.S. designed the experiments and carried out the work. E.H., E.K., N.B., Y.Y., M.W., M.C.B., H.U. ,and R.S. wrote the article under guidance from G.C., M.J., A.W., J.G., and S.J.D.

Received November 15, 2011; revised November 15, 2011; accepted January 20, 2012; published February 10, 2012.

REFERENCES

Alabadí, D., Oyama, T., Yanovsky, M.J., Harmon, F.G., Más, P., and Kay, S.A. (2001). Reciprocal regulation between TOC1 and LHY/CCA1 within the Arabidopsis circadian clock. Science **293:** 880–883.

Brudno, M., Malde, S., Poliakov, A., Do, C.B., Couronne, O., Dubchak, I., and Batzoglou, S. (2003). Glocal alignment: finding rearrangements during alignment. Bioinformatics **19** (suppl. 1): i54–i62.

Chen, M. (2008). Phytochrome nuclear body: An emerging model to study interphase nuclear dynamics and signaling. Curr. Opin. Plant Biol. **11:** 503–508.

Chen, M., Galvão, R.M., Li, M., Burger, B., Bugea, J., Bolado, J., and Chory, J. (2010). Arabidopsis HEMERA/pTAC12 initiates photomorphogenesis by phytochromes. Cell **141:** 1230–1240.

Covington, M.F., Maloof, J.N., Straume, M., Kay, S.A., and Harmer, S. L. (2008). Global transcriptome analysis reveals circadian regulation of key pathways in plant growth and development. Genome Biol. **9:** R130.

Covington, M.F., Panda, S., Liu, X.L., Strayer, C.A., Wagner, D.R., and Kay, S.A. (2001). ELF3 modulates resetting of the circadian clock in *Arabidopsis*. Plant Cell **13:** 1305–1315.

Crooks, G.E., Hon, G., Chandonia, J.M., and Brenner, S.E. (2004). WebLogo: A sequence logo generator. Genome Res. **14:** 1188–1190.

Dalchau, N., Hubbard, K.E., Robertson, F.C., Hotta, C.T., Briggs, H.M., Stan, G.B., Gonçalves, J.M., and Webb, A.A. (2010). Correct biological timing in Arabidopsis requires multiple light-signaling pathways. Proc. Natl. Acad. Sci. USA **107:** 13171–13176.

Davis, A.M., Hall, A., Millar, A.J., Darrah, C., and Davis, S.J. (2009). Protocol: Streamlined sub-protocols for floral-dip transformation and selection of transformants in *Arabidopsis thaliana*. Plant Methods **5:** 3.

Davis, S.J. (2002). Photoperiodism: The coincidental perception of the season. Curr. Biol. **12:** R841–R843.

Davis, S.J., and Millar, A.J. (2001). Watching the hands of the Arabidopsis biological clock. Genome Biol. **2:** 1008.1–1008.4.

Devlin, P.F., and Kay, S.A. (2000). Cryptochromes are required for phytochrome signaling to the circadian clock but not for rhythmicity. Plant Cell **12:** 2499–2510.

Ding, Z., Doyle, M.R., Amasino, R.M., and Davis, S.J. (2007). A complex genetic interaction between *Arabidopsis thaliana* TOC1 and CCA1/LHY in driving the circadian clock and in output regulation. Genetics **176:** 1501–1510.

Dixon, L.E., Knox, K., Kozma-Bognar, L., Southern, M.M., Pokhilko, A., and Millar, A.J. (2011). Temporal repression of core circadian genes is mediated through EARLY FLOWERING 3 in Arabidopsis. Curr. Biol. **21:** 120–125.

Dodd, A.N., Salathia, N., Hall, A., Kévei, E., Tóth, R., Nagy, F., Hibberd, J.M., Millar, A.J., and Webb, A.A. (2005). Plant circadian clocks increase photosynthesis, growth, survival, and competitive advantage. Science **309:** 630–633.

Doyle, M.R., Davis, S.J., Bastow, R.M., McWatters, H.G., Kozma-Bognár, L., Nagy, F., Millar, A.J., and Amasino, R.M. (2002). The ELF4 gene controls circadian rhythms and flowering time in *Arabidopsis thaliana*. Nature **419:** 74–77.

Fowler, S., Lee, K., Onouchi, H., Samach, A., Richardson, K., Morris, B., Coupland, G., and Putterill, J. (1999). GIGANTEA: A circadian clock-controlled gene that regulates photoperiodic flowering in Arabidopsis and encodes a protein with several possible membrane-spanning domains. EMBO J. **18:** 4679–4688.

Graf, A., Schlereth, A., Stitt, M., and Smith, A.M. (2010). Circadian control of carbohydrate availability for growth in Arabidopsis plants at night. Proc. Natl. Acad. Sci. USA **107:** 9458–9463.

Hajdukiewicz, P., Svab, Z., and Maliga, P. (1994). The small, versatile pPZP family of Agrobacterium binary vectors for plant transformation. Plant Mol. Biol. **25:** 989–994.

Hanano, S., Domagalska, M.A., Nagy, F., and Davis, S.J. (2006). Multiple phytohormones influence distinct parameters of the plant circadian clock. Genes Cells **11:** 1381–1392.

Hanano, S., Stracke, R., Jakoby, M., Merkle, T., Domagalska, M.A., Weisshaar, B., and Davis, S.J. (2008). A systematic survey in *Arabidopsis thaliana* of transcription factors that modulate circadian parameters. BMC Genomics **9:** 182.

Harmer, S.L. (2009). The circadian system in higher plants. Annu. Rev. Plant Biol. **60:** 357–377.

Harmer, S.L., Hogenesch, J.B., Straume, M., Chang, H.S., Han, B., Zhu, T., Wang, X., Kreps, J.A., and Kay, S.A. (2000). Orchestrated transcription of key pathways in Arabidopsis by the circadian clock. Science **290:** 2110–2113.

Hazen, S.P., Schultz, T.F., Pruneda-Paz, J.L., Borevitz, J.O., Ecker, J.R., and Kay, S.A. (2005). LUX ARRHYTHMO encodes a Myb domain protein essential for circadian rhythms. Proc. Natl. Acad. Sci. USA **102:** 10387–10392.

Helfer, A., Nusinow, D.A., Chow, B.Y., Gehrke, A.R., Bulyk, M.L., and Kay, S.A. (2011). LUX ARRHYTHMO encodes a nighttime repressor of circadian gene expression in the Arabidopsis core clock. Curr. Biol. **21:** 126–133.

Herrero, E., and Davis, S.J. (2012). Time for a nuclear meeting: Protein trafficking and chromatin dynamics intersect in the plant circadian system. Mol. Plant, in press.

Hicks, K.A., Albertson, T.M., and Wagner, D.R. (2001). EARLY FLOWERING3 encodes a novel protein that regulates circadian clock function and flowering in *Arabidopsis*. Plant Cell **13:** 1281–1292.

Hicks, K.A., Millar, A.J., Carré, I.A., Somers, D.E., Straume, M., Meeks-Wagner, D.R., and Kay, S.A. (1996). Conditional circadian dysfunction of the Arabidopsis early-flowering 3 mutant. Science **274:** 790–792.

Hung, H.C., Maurer, C., Zorn, D., Chang, W.L., and Weber, F. (2009). Sequential and compartment-specific phosphorylation controls the life cycle of the circadian CLOCK protein. J. Biol. Chem. **284:** 23734–23742.

Ito, S., Nakamichi, N., Matsushika, A., Fujimori, T., Yamashino, T., and Mizuno, T. (2005). Molecular dissection of the promoter of the light-induced and circadian-controlled APRR9 gene encoding a clock-associated component of *Arabidopsis thaliana*. Biosci. Biotechnol. Biochem. **69:** 382–390.

Khanna, R., Kikis, E.A., and Quail, P.H. (2003). EARLY FLOWERING 4 functions in phytochrome B-regulated seedling de-etiolation. Plant Physiol. **133:** 1530–1538.

Kikis, E.A., Khanna, R., and Quail, P.H. (2005). ELF4 is a phytochrome-regulated component of a negative-feedback loop involving the central oscillator components CCA1 and LHY. Plant J. **44:** 300–313.

Kolmos, E., and Davis, S.J. (2007). ELF4 as a central gene in the circadian clock. Plant Signal. Behav. **2:** 370–372.

Kolmos, E., Herrero, E., Bujdoso, N., Millar, A.J., Tóth, R., Gyula, P., Nagy, F., and Davis, S.J. (2011). A reduced-function allele reveals that EARLY FLOWERING3 repressive action on the circadian clock is modulated by phytochrome signals in *Arabidopsis*. Plant Cell **23:** 3230–3246.

Kolmos, E., Nowak, M., Werner, M., Fischer, K., Schwarz, G., Mathews, S., Schoof, H., Nagy, F., Bujnicki, J.M., and Davis, S.J. (2009). Integrating ELF4 into the circadian system through combined structural and functional studies. Front. Life Sci. (formerly HFSP J.) **3:** 350–366.

Kondratov, R.V., Chernov, M.V., Kondratova, A.A., Gorbacheva, V.Y., Gudkov, A.V., and Antoch, M.P. (2003). BMAL1-dependent circadian oscillation of nuclear CLOCK: Posttranslational events induced by dimerization of transcriptional activators of the mammalian clock system. Genes Dev. **17:** 1921–1932.

Li, G., et al. (2011). Coordinated transcriptional regulation underlying the circadian clock in Arabidopsis. Nat. Cell Biol. **13:** 616–622.

Liu, X.L., Covington, M.F., Fankhauser, C., Chory, J., and Wagner, D.R. (2001). ELF3 encodes a circadian clock-regulated nuclear protein that functions in an *Arabidopsis* PHYB signal transduction pathway. Plant Cell **13:** 1293–1304.

Locke, J.C., Kozma-Bognár, L., Gould, P.D., Fehér, B., Kevei, E., Nagy, F., Turner, M.S., Hall, A., and Millar, A.J. (2006). Experimental validation of a predicted feedback loop in the multi-oscillator clock of *Arabidopsis thaliana*. Mol. Syst. Biol. **2:** 59.

Lu, S.X., Webb, C.J., Knowles, S.M., Kim, S.H.J., Wang, Z., and Tobin, E.M. (2012). CCA1 and ELF3 interact in the control of hypocotyl length and flowering time in Arabidopsis. Plant Physiol.**158:** 1079–1088.

Más, P., Devlin, P.F., Panda, S., and Kay, S.A. (2000). Functional interaction of phytochrome B and cryptochrome 2. Nature **408:** 207–211.

Matsumoto, A., et al. (2007). A functional genomics strategy reveals clockwork orange as a transcriptional regulator in the Drosophila circadian clock. Genes Dev. **21:** 1687–1700.

Mayor, C., Brudno, M., Schwartz, J.R., Poliakov, A., Rubin, E.M., Frazer, K.A., Pachter, L.S., and Dubchak, I. (2000). VISTA : visualizing global DNA sequence alignments of arbitrary length. Bioinformatics **16:** 1046–1047.

McWatters, H.G., Bastow, R.M., Hall, A., and Millar, A.J. (2000). The ELF3 zeitnehmer regulates light signalling to the circadian clock. Nature **408:** 716–720.

McWatters, H.G., Kolmos, E., Hall, A., Doyle, M.R., Amasino, R.M., Gyula, P., Nagy, F., Millar, A.J., and Davis, S.J. (2007). ELF4 is required for oscillatory properties of the circadian clock. Plant Physiol. **144:** 391–401.

Michael, T.P., et al. (2008). Network discovery pipeline elucidates conserved time-of-day-specific cis-regulatory modules. PLoS Genet. **4:** e14.

Morgenstern, B. (2004). DIALIGN: Multiple DNA and protein sequence alignment at BiBiServ. Nucleic Acids Res. **32**(Web Server issue): W33–W36.

Nakamichi, N., Kiba, T., Henriques, R., Mizuno, T., Chua, N.H., and Sakakibara, H. (2010). PSEUDO-RESPONSE REGULATORS 9, 7, and 5 are transcriptional repressors in the *Arabidopsis* circadian clock. Plant Cell **22:** 594–605.

Nusinow, D.A., Helfer, A., Hamilton, E.E., King, J.J., Imaizumi, T., Schultz, T.F., Farré, E.M., and Kay, S.A. (2011). The ELF4-ELF3-LUX complex links the circadian clock to diurnal control of hypocotyl growth. Nature **475:** 398–402.

Oka, Y., Matsushita, T., Mochizuki, N., Quail, P.H., and Nagatani, A. (2008). Mutant screen distinguishes between residues necessary for light-signal perception and signal transfer by phytochrome B. PLoS Genet. **4:** e1000158.

Onai, K., and Ishiura, M. (2005). PHYTOCLOCK 1 encoding a novel GARP protein essential for the Arabidopsis circadian clock. Genes Cells **10:** 963–972.

Perales, M., and Más, P. (2007). A functional link between rhythmic changes in chromatin structure and the *Arabidopsis* biological clock. Plant Cell **19:** 2111–2123.

Pokhilko, A., Hodge, S.K., Stratford, K., Knox, K., Edwards, K.D., Thomson, A.W., Mizuno, T., and Millar, A.J. (2010). Data assimilation constrains new connections and components in a complex, eukaryotic circadian clock model. Mol. Syst. Biol. **6:** 416.

Quail, P.H. (2000). Phytochrome-interacting factors. Semin. Cell Dev. Biol. **11:** 457–466.

Roden, L.C., and Ingle, R.A. (2009). Lights, rhythms, infection: The role of light and the circadian clock in determining the outcome of plant-pathogen interactions. Plant Cell **21:** 2546–2552.

Schaffer, R., Ramsay, N., Samach, A., Corden, S., Putterill, J., Carré, I.A., and Coupland, G. (1998). The late elongated hypocotyl mutation of Arabidopsis disrupts circadian rhythms and the photoperiodic control of flowering. Cell **93:** 1219–1229.

Thines, B., and Harmon, F.G. (2010). Ambient temperature response establishes ELF3 as a required component of the core Arabidopsis circadian clock. Proc. Natl. Acad. Sci. USA **107:** 3257–3262.

Ukai-Tadenuma, M., Kasukawa, T., and Ueda, H.R. (2008). Proof-by-synthesis of the transcriptional logic of mammalian circadian clocks. Nat. Cell Biol. **10:** 1154–1163.

Ukai-Tadenuma, M., Yamada, R.G., Xu, H., Ripperger, J.A., Liu, A.C.,

and Ueda, H.R. (2011). Delay in feedback repression by cryptochrome 1 is required for circadian clock function. Cell **144:** 268–281.

Untergasser, A., Nijveen, H., Rao, X., Bisseling, T., Geurts, R., and Leunissen, J.A. (2007). Primer3Plus, an enhanced web interface to Primer3. Nucleic Acids Res. **35**(Web Server issue): W71–W74.

Voinnet, O., Rivas, S., Mestre, P., and Baulcombe, D. (2003). An enhanced transient expression system in plants based on suppression of gene silencing by the p19 protein of tomato bushy stunt virus. Plant J. **33:** 949–956.

Wang, L., Fujiwara, S., and Somers, D.E. (2010). PRR5 regulates phosphorylation, nuclear import and subnuclear localization of TOC1 in the Arabidopsis circadian clock. EMBO J. **29:** 1903–1915.

Yu, J.W., et al. (2008). COP1 and ELF3 control circadian function and photoperiodic flowering by regulating GI stability. Mol. Cell **32:** 617–630.

Zeilinger, M.N., Farre, E.M., Taylor, S.R., Kay, S.A., and Doyle, F.J. (2006). A novel computational model of the circadian clock in Arabidopsis that incorporates PRR7 and PRR9. Mol. Syst. Biol. **2:** 58.

EARLY FLOWERING4 Recruitment of EARLY FLOWERING3 in the Nucleus Sustains the *Arabidopsis* Circadian Clock

Eva Herrero, Elsebeth Kolmos, Nora Bujdoso, Ye Yuan, Mengmeng Wang, Markus C. Berns, Heike Uhlworm, George Coupland, Reena Saini, Mariusz Jaskolski, Alex Webb, Jorge Gonçalves and Seth J. Davis

Plant Cell; originally published online February 10, 2012;
DOI 10.1105/tpc.111.093807